i shallow donors band, a second tre and ice behavior is ter and Mg is

/ for helpful NAG5-1147 (P. Science and

Story (Springer,

IEĖE J.

, **68**, 1808 (1996). ppl. Phys. Lett.,

. 1639 (1990). Furnbull, and S.

G6.39.1 (2001).

)5 (1998). ), G6.39.1 (2001).

999).

ty Fall Meeting,

ጋ).

. Lim, Solid

Appl. Phys., 84,

# Dielectric Function of "Narrow" Band Gap InN

R. Goldhahn<sup>1</sup>, S. Shokhovets<sup>1</sup>, V. Cimalla<sup>2</sup>, L. Spiess<sup>2</sup>, G. Ecke<sup>2</sup>, O. Ambacher<sup>2</sup>,

J. Furthmüller<sup>3</sup>, F. Bechstedt<sup>3</sup>, H. Lu<sup>4</sup> and W.J. Schaff<sup>4</sup>

<sup>1</sup>Institute of Physics and <sup>2</sup>Center for Micro- and Nanotechnologies,

Technical University Ilmenau, 98684 Ilmenau, Germany

<sup>3</sup>Institut of Solid State Theory and Theoretical Optics, Friedrich Schiller University, 07743 Jena, Germany

<sup>4</sup>Departartment of Electrical and Computer Engineering, Cornell University, Ithaca, NY 14853, U.S.A.

#### **ABSTRACT**

. Spectroscopic ellipsometry studies in the energy range from 0.7 up to 5.5 eV were carried out in order to determine the dielectric function (DF) of 'narrow' band gap (< 1 eV) single-crystalline InN films grown by molecular beam epitaxy on sapphire substrates. The imaginary part of the DF is characterized by a strong increase immediately above the band gap and then by a nearly constant value up to 4 eV. Pronounced structures above 4 eV are attributed to transitions along the L-M direction in the Brillouin-zone as a comparison with *first-principles* calculations indicates. In contrast, sputtered layers (band gap ~1.9 eV) studied for comparison show a completely different spectral shape of the DF. Finally, DF's of high In-content InGaN alloys are presented, providing further evidence that InN is a "narrow" band gap semiconductor.

#### INTRODUCTION

Among the group-III nitride semiconductor compounds, the physical properties of InN are known rather poorly. This is mainly attributed to the difficulties in growing high-quality crystals. A discussion of optical properties of InN demands to differentiate between investigations employing either sputtered films or epitaxial layers deposited by molecular beam epitaxy (MBE) and metalorganic vapor-phase epitaxy (MOVPE). Interband optical absorption measurements of sputtered polycrystalline InN films yield a band gap of  $E_e$ -1.9 eV at room temperature [1-4]. This value of the band gap has been accepted for a long time and was frequently used as the endpoint value for the extrapolation of the band gap in  $In_xGa_{1-x}N$  alloys. In contrast, recent studies of epitaxial layers grown by MBE [5-7] or MOVPE [8] revealed a narrow gap of  $E_e$ <1 eV.

For both types of films, reports on the dielectric function (DF) covering an extended energy range are scarce. Refractive index and extinction coefficient of sputtered layers were obtained from transmittance/reflectance [3] and spectroscopic ellipsometry (SE) [9] studies. However, the applied single-layer model neglects the influence of roughness and interface layers on the spectra [10]. Guo et al. reported optical constants for MOVPE grown InN determined from reflectance investigations followed by Kramers-Kronig analysis. These data suffer from the relatively low InN layer thickness (~300 nm) and the neglect of sample surface roughness. However, both effects require the application of a multi-layer model.

In this work, we present a comprehensive SE data analysis based on multi-layer models in order to determine the InN DF's for both single-crystalline MBE grown and sputtered films with high reliability. The extracted data are compared with the results of *first-principles* calculations.

The single-crystalline InN films were grown on (0001) sapphire by MBE as described elsewhere [12]. For two samples the InN layers of 120 nm (#M1) and 250 nm (#M2) thickness (nominal) were directly deposited on top of an 230 nm AlN buffer layer. The third sample (#M3) consists of a 10 nm AlN nucleation layer followed by a 310 nm GaN buffer layer and the final 960 nm InN film. Structural properties of the films were examined by high resolution x-ray diffraction (HRXRD) measurements. For all samples, the optical axis (c) is oriented normal to the surface. From reciprocal space maps of the symmetric (002) and the asymmetric (20.5) Bragg reflexes the InN lattice constants were determined. For sample #M3 we found c = 5.686 Å and a = 3.552 Å which is in excellent agreement with previous studies of thick InN films deposited on GaN [13]. The lattice constants of the other two samples deviate only slightly from these values. The root-mean-square (rms) surface roughness δ was obtained by atomic force microscopy (AFM) yielding  $\delta = 9$ , 1.5, and 12 nm for samples #M1, #M2, and M#3. respectively. Hall measurements at room temperature evidenced for the thinner samples electron. densities (mobilities) of ~2x10<sup>18</sup> cm<sup>-3</sup> (~850 cm<sup>2</sup>/Vs) and for the thicker sample of 8x10<sup>17</sup> cm<sup>-3</sup>  $(1500 \text{ cm}^2/\text{Vs})$ .

In order to demonstrate the systematic change of the DF with increasing Ga-content, three  $In_{1-x}Ga_xN$  alloys (x = 0.22, 0.32, and 0.43) with thickness of ~250 nm were grown by MBE on sapphire substrates with an AlN buffer layer (~250 nm) [4]. The growth temperature was in the range of 470 to 570 °C. The Ga atomic fraction was determined by XRD assuming a complete lattice relaxation.

The polycrystalline lnN layers under investigation were provided by the Tansley group. They were deposited by magnetron sputtering of a nitrided indium target in a reactive nitrogen plasma [3] either on glass (#S1) or Si (#S2) substrates with a thickness of 975 nm and 1210 nm. respectively. The layers are composed of needle-like crystallites with diameters in the range of 10-30 nm. The lattice constants of #S1 (#S2) are c = 5.821 Å (5.786 Å) and a = 3.622 Å(3.58 Å). For both samples the roughness amounts to  $\delta \sim 8$  nm.

The optical properties of the films were investigated by SE. In order to minimize the correlation between DF's and layer thickness, the ellipsometric parameters  $\Psi$  and  $\Delta$  were measured at different angles of incidence (60°, 68°, and 74°).

### RESULTS AND DISCUSSION

The dots in Fig. 1(a) and (b) represent typical examples for the spectral dependence of the ellipsometric parameter Y taken at different angles of incidence for the thick single-crystalline film #M3 and the sputtered layer on Si substrate #S2. Remarkable differences are observed. For the sputtered layer in Fig. 1(b),  $\Psi$  shows oscillatory behavior below ~2 eV due to interference, but a smooth dependence on the photon energy at higher energy. Obviously, the film is transparent in the low-energy range and strongly absorbing above 2 eV. In contrast, for the MBE grown film oscillations start to evolve only below ~1 eV indicating a much smaller band gap for this film. It is worth noting that  $\Delta$ , not presented here, shows similar features.

A multi-layer model has been established for determining the real  $(\varepsilon_1)$  and imaginary  $(\varepsilon_2)$ part of the complex DF ( $\bar{\epsilon} = \epsilon_1 + i \cdot \epsilon_2$ ) from the experimental data. For the MBE samples, it consists of the substrate, buffer layer, InN film, and a surface layer. The latter takes into account the sample surface roughness. Its optical constants are modeled by an effective medium theory 30

30 25

20

15

40

samples fitted to averaged Such an it minim range. It the DF ( lines in l over the assumpti layers th example

assuming

demonst

Belg in the fo density f ab-initio guarante were cal-MBE gr gap of I optical p 3E as described (#M2) thickness id sample (#M3) yer and the final resolution x-ray iented normal to tric (20.5) Bragg c = 5.686 Å and films deposited ghtly from these by atomic force fM2, and M#3, samples electron e of 8x10<sup>17</sup> cm<sup>-3</sup>

Fa-content, three own by MBE on rature was in the ming a complete

Tansley group. reactive nitrogen m and 1210 nm, s in the range of and a = 3.622 Å

to minimize the  $\Psi$  and  $\Delta$  were

pendence of the single-crystalline re observed. For to interference, sly, the film is ast, for the MBE ller band gap for

d imaginary ( $\varepsilon_2$ )
ABE samples, it kes into account medium theory

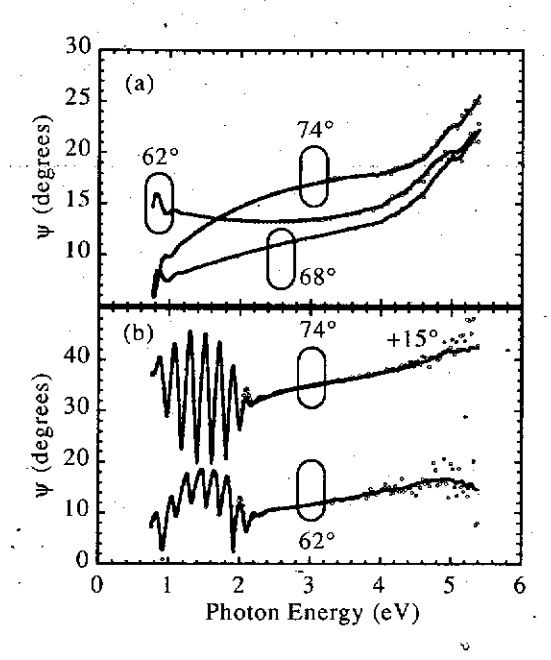


Figure 1.
Fit (full lines) of ellipsometric data (dots) taken at different angles of incidence. (a) and (b) refer to the MBE grown single-crystalline InN film (#M3) and InN obtained by sputtering techniques (#S2), respectively. Data taken at 74° in (b) are shifted by 15° for clarity.

assuming a 1/1 mixture of InN with voids. The applicability of this method has been demonstrated in Ref. 10. Furthermore, we assumed that the DF of InN should be identical for all samples of the M series, i.e. the data of all samples ( $\Psi$  and  $\Delta$  at various angles of incidence) are fitted together for determining one pair of  $\epsilon_1$  and  $\epsilon_2$  values at each photon energy yielding an averaged DF. The layer thicknesses were allowed to vary with respect to the nominal values. Such an approach (point-by-point multi-sample fit) increases the reliability of the  $\overline{\epsilon}$  data because it minimizes the correlation to the layer thickness and removes the noise in the high-energy range. It should be noticed again that we did not make any assumption concerning the shape of the DF (dielectric function model). The fit results for  $\Psi$  of sample #M3 are indicated by the full lines in Fig. 1(a). In this example as well as for the other spectra, excellent agreement is obtained over the full investigated range although the averaged DF is employed. It emphasizes the assumption of a, within the experimental uncertainty, sample independent DF. For the sputtered layers the multi-sample fit yields similar good agreement with the experimental data as the example in Fig. 1(b) demonstrates.

Before discussing the extracted DF's, a-few-details of the theoretical calculations are given in the following. The properties of wurtzite InN have been calculated within the framework of density functional theory (DFT) in its local density approximation (LDA) employing the Vienna ab-initio Simulation Package [14]. The In4d electrons are treated as valence electrons. It guarantees correct structural properties, and lattice constants of c = 5.688 Å and a = 3.523 Å were calculated. Besides the strain aspects, these values agree well with the data obtained for the MBE grown layers. This DFT-LDA procedure, however, gives a negative fundamental energy gap of InN because p-d repulsion is strongly overestimated. In the case of calculations of the optical properties, we therefore used another type of pseudopotentials which account for self-

compa essenti part in above. from t [18]. ] proced two ty energe like In

this co not cha increas to high energy

In analysi sputter MBE s

interaction corrections of the 4d electrons in the underlying atomic calculation but freeze the In4d electrons in the core [15]. Already in the DFT-LDA case this opens artificially a gap. Therefore, additional quasi-particle corrections (overestimating the gap) were not taken into account in the calculations of optical properties. The independent-particle approximation and the projector-augmented-wave (PAW) method [16] are applied to calculate at first the imaginary part of the dielectric function [17]. The real part of the dielectric function is obtained via a Kramers-Kronig transform.

Fig. 2 summarizes the optical properties for InN concerning the real (a) and imaginary (b) parts of the DF as well as for the corresponding absorption coefficient  $\alpha$  (c). The full and dashed lines are obtained by the point-by-point multi-sample fits of the MBE grown (M series) and sputtered (S series) films, respectively, while the long-dashed lines represent the results of the DFT-LDA calculations. Let us first focus on the absorption coefficient (c). Our results for the sputtered films are in excellent agreement with previous investigations [2]. Those layers show only weak absorption in the energy range between 1 and 2 eV. For single-crystalline InN, however, the absorption coefficient increases continuously with the photon energy.

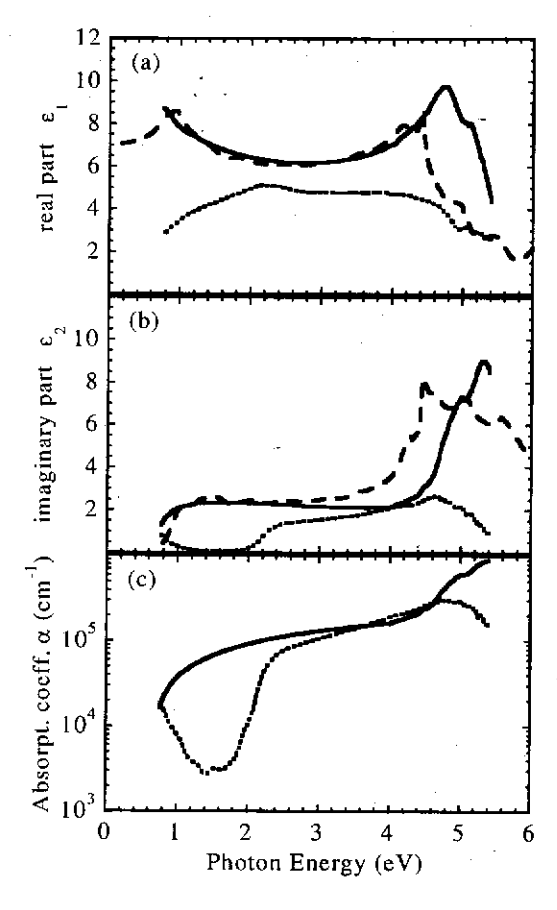


Figure 2. Comparison of the real (a) and imaginary (b) part of the DF and the absorption coefficient for InN. The full and dashed lines are obtained from the by point-bypoint multi-sample fits of the MBE grown (M series) and sputtered (S series) layers, respectively. The long-dashed lines represent the results of the calculations without quasi-particle corrections.

n but freeze the rtificially a gap. e not taken into ximation and the le imaginary part d via a Kramers-

id imaginary (b) e full and dashed (M series) and he results of the ir results for the lose layers show-crystalline InN, ty-

ne real (a) and t of the DF and fficient for InN. shed lines are e by point-by-le fits of the A series) and series) layers, e long-dashed e results of the ut quasi-particle

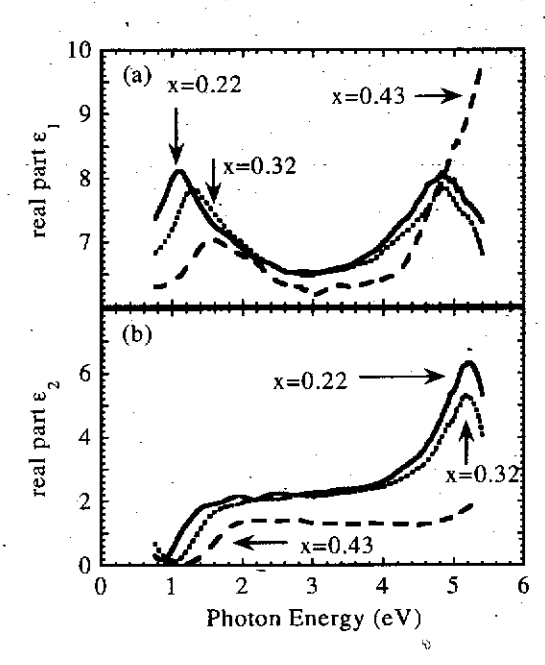


Figure 3. Real (a) and imaginary (b) part of the DF for In<sub>1-x</sub>Ga<sub>x</sub>N alloys obtained from fitting ellipsometric data.

The main result of this work is shown in Fig. 2(b) where the imaginary parts of the DF's are compared. The MBE grown films exhibit a spectral dependence of  $\epsilon_2$  which coincides in essential features with the theoretical results. Above the band gap ( $E_g \approx 0.75 \text{ eV}$ ) the imaginary part increases very sharply indicating a non-parabolic band structure and remains nearly constant above the band gap up to energies of about 4 eV. The strong increase at higher energies arise from transitions along the L-M direction in the Brillouin-zone and was also calculated in Ref. [18]. However, its energetic position depends on the assumptions made in the DFT-LDA procedure. For the sputtered films such a strong increase around 4 eV is not observed, i.e. the two types of InN films differ not only in their band gap values but in addition in the higher-energetic parts of the DF. Therefore we conclude that only the MBE grown films represent bulk-like InN in the wurtzite structure.

Preliminary results of ellipsometry studies on  $In_{1-x}Ga_xN$  films shown in Fig. 3 emphasize this conclusion. As expected for an alloy system the spectral shape of both parts of the DF does not change very much if a low amount of Ga atoms replace In atoms in the InN lattice. With increasing Ga-content the step-like structure of  $\varepsilon_2$  found between 1 and 2 eV shifts continuously to higher energies reflecting the rising band gaps. But even for 43% Ga composition, the gap energy is unambiguously below 1.9 eV, the value reported for sputtered films

In summary, applying spectroscopic ellipsometry and using multi-layer models for data analysis, we have determined the complex dielectric function from the near infra-red up to the near ultra-violet spectral region for single-crystalline InN films grown by MBE as well as of sputtered polycrystalline InN layers. Striking differences of the optical properties were found. MBE grown InN films show a 'narrow' band gap of around 0.75 eV, a nearly photon energy

independent imaginary part of the DF between 1 and 4 eV, and a strongly enhanced transition probability above 4 eV. The qualitative behavior agrees in essential features with the presented results of theoretical predictions. In contrast, sputtered layers with a gap energy around 1.9 eV do not show the increase of  $\epsilon_2$  at higher energies. Therefore, we conclude that 'narrow' band gap InN obtained by epitaxial growth techniques represents InN in the wurtzite structure with bulk-like properties. The clarification of the deviating properties of sputtered films requires further studies.

#### **ACKNOWLEDGEMENTS**

The authors would like to thank the group of T.L. Tansley for providing the sputtered InN film for optical studies. The groups from Ilmenau University acknowledge financial support by the Thuringia Ministry of Science, Research, and Art under contract No. B609-02004. The work at Cornell University is supported by ONR Contract No. N000149910936 monitored by Dr. C. Wood.

## REFERENCES

- K. Osamura, K. Nakajima, Y. Murakami, P. S. Shingu and A. Ohtsuki, Solid State Commun. 11, 617 (1972); K. Osamura, S. Naka and Y. Murakami, J. Appl. Phys. 46, 3432 (1975).
- 2. T.L. Tansley and C.P. Fowley, J. Appl. Phys. 59, 3241 (1986).
- 3. R.T. Shamrell and C. Parman, Optical Materials 13, 289 (1999).
- W. Z. Shen et al., Appl. Phys. Lett. 80, 2063 (2002); H. F. Yang et al., J. Appl. Phys. 91, 9803 (2002).
- T. Inushima, V. V. Mamutin, V.A. Vekshin, S. V. Ivanov, T. Sakon, M. Motokawa and S. Ohoya, J. Crytal Growth 227-228, 481 (2001).
- 6. V. Yu. Davydov et al., phys. stat. sol. (b) 229, R1 (2002).
- 7. J. Wu et al., Appl. Phys. Lett. 80, 3967 (2002); J. Wu et al., ibid. 80, 4741 (2002).
- T. Matsuoka, H. Okamoto, M. Nakao, H. Harima and E. Kurimoto, Appl. Phys. Lett. 81, 1246 (2002).
- F. Li, D. Mo, C. B. Cao, Y. L. Zhang, H. L. Chan and C. L. Choy, J. Mat. Science: Mat. in Electronics 12, 725 (2001).
- 10. R. Goldhahn et al., phys. stat. sol. (a) 177, 107 (2001)
- Q. Guo, O. Kato, M. Fujisawa and A. Yoshida, Solid State Commun. 83, 721 (1992);
   Q. Guo, H. Ogawa and A. Yoshida, J. Electron Spectrosc. Relat. Phenom. 79, 9 (1996).
- H. Lu, W. J. Schaff, J. Hwang, H. Wu, G. Koley and L. F. Eastman, Appl. Phys. Lett. 79, 1489 (2001).
- S. Yamaguchi, M. Kariya, S. Nitta, T. Takeuchi, C. Wetzel, H. Amano and I. Akasaki, J. Appl. Phys. 85, 7682 (1999).
- G. Kresse and J. Furthmüller, Comput. Mater. Sci. 6, 15 (1996); Phys. Rev. B 54, 11169 (1996).
- 15. M. M. Rieger and P. Vogl, Phys. Rev. B 52, 16567 (1995).
- 16. G. Kresse and D. Joubert, Phys. Rev. B 59, 1758 (1999).
- 17. B. Adolph, J. Furthmüller and F. Bechstedt, Phys. Rev. B 63, 125108 (2001).
- C. Persson, R. Ahuja, A. Ferreira da Silva and B. Johansson, J. Phys.: Condens. Matter 13, 8945 (2001).